Mendeleev Communications

Mendeleev Commun., 2025, **35**, 566–568

Synthesis of nanosized HZSM-5 zeolite under microwave irradiation: effect of the Si/Al ratio on the morphology, textural and acidic properties

Alexander A. Karavaev,*[a] Kirill A. Cherednichenko,[b] Evgenya R. Koroleva,[b] Alexander A. Panin[c] and Leonid M. Kustov[a]

[a] *N. D. Zelinsky Institute of Organic Chemistry, Russian Academy of Sciences, 119991 Moscow, Russian Federation. E-mail: aleksankarav@yandex.ru*

[b] *National University of Oil and Gas 'Gubkin University', 119991 Moscow, Russian Federation*

[c] *A. V. Topchiev Institute of Petrochemical Synthesis, Russian Academy of Sciences, 119991 Moscow, Russian Federation*

DOI: 10.71267/mencom.7751

The effect of the Si/Al ratio on morphology, textural and acidic properties of nanosized ZSM-5 zeolite synthesized by the one-stage microwave hydrothermal method directly in a proton form has been established. The materials were characterized by the X-ray diffraction, scanning electron microscopy, transmission electron microscopy, N_2 sorption, inductively coupled plasma optical emission spectrometry (ICP-OES) and thermal desorption of ammonia. It was found that with a decrease in the Si/Al ratio from 270 to 46, the total acidity increases from 90 to 542 μmol g^{-1} and the particle size decreases from 150 to 15–25 nm; at the same time, the particles assemble into larger aggregates.

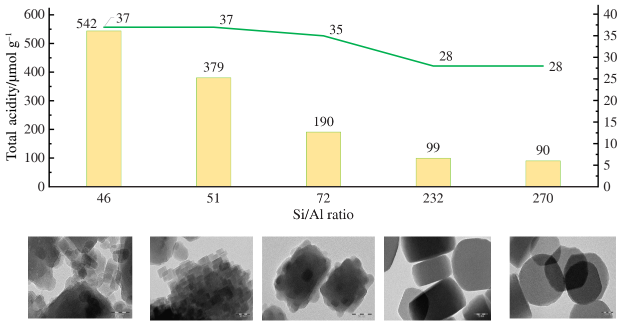

Keywords: nanosized ZSM-5 zeolite, microwave hydrothermal synthesis, Si/Al ratio, proton form, morphology, acidity, interparticle porosity, micro/mesopores.

ZSM-5 zeolites are widely used in various acid–base catalytic processes, in particular, in petrochemistry and oil and gas processing.[1–10] Nanosized zeolites are of particular interest due to their higher external specific surface area and smaller crystal size, which makes it possible to improve access to active centers in micropores and minimize diffusion limitations.[11–18]

The physico-chemical properties of ZSM-5 zeolite depend on the synthesis method, sources of silicon and aluminum, temperature and synthesis time and the ratio of reagents. One of the key parameters affecting the physico-chemical properties of zeolites is the silica module (Si/Al ratio). The Si/Al ratio determines the concentration and location of aluminum tetrahedra, and, consequently, the strength and concentration of Brønsted acid centers.[19] However, a number of studies have shown that the Si/Al ratio affects not only the acidic properties of zeolites, but also the morphology and porous structure.[20–26] Morphology and textural properties play a key role in the zeolite catalysis: catalytic activity, product selectivity, catalytic stability, and they can be enhanced.[21–23]

The use of microwave hydrothermal technique for the zeolite synthesis can significantly reduce the synthesis time, increase the uniformity of the structure and particle size and improve the dissolution of the precursor gel.[27] The effect of the Si/Al ratio on the properties of ZSM-5 zeolite synthesized by the microwave hydrothermal method with micron-sized particles[23] and with nanoscale particles[28] has been described. The authors[28] carried out two-stage crystallization to obtain particles with the size of 180–300 nm. They found that as the Si/Al ratio increases, the particle size decreases. At the same time, there is no data on the acidic and textural properties of the obtained zeolites. Earlier,[29] the possibility of obtaining nanosized ZSM-5 zeolite *via* the microwave hydrothermal method with one-stage crystallization directly in a proton form with a predominance of particles with the size of 30–80 nm was shown.

In this paper, we report for the first time the effect of the Si/Al ratio on the morphology, textural and acidic properties of nanosized ZSM-5 zeolite synthesized *via* microwave hydrothermal method directly in a proton form with one-stage crystallization.

The molar ratio of reagents $Si(OEt)_4 : H_2O : TPA–OH : Al(OPr^i)_3$ is presented in Table 1.

All synthesized samples were crystalline ZSM-5 zeolites without other phases (Figure 1), as it was confirmed by XRD. The presence of characteristic peaks in the 2θ ranges of 8–9 and 23–25° proves the crystalline structure of the synthesized ZSM-5 zeolite according to the ICDD database.

Table 1 Molar ratio of the reagents and Si/Al ratio in the synthesized ZSM-5 zeolites.

Sample	Gel composition (mol)[a]	Si/Al molar ratio[b]
nanoHZSM-5_46	1 : 8.3 : 0.47 : 0.015	46
nanoHZSM-5_51	1 : 8.3 : 0.47 : 0.011	51
nanoHZSM-5_72	1 : 6.1 : 0.34 : 0.008	72
nanoHZSM-5_232	1 : 4.47 : 0.26 : 0.0045	232
nanoHZSM-5_270	1 : 4.47 : 0.26 : 0.003	270

[a] The molar ratio of reagents $Si(OEt)_4 : H_2O : TPA–OH : Al(OPr^i)_3$.
[b] Determined by ICP-OES.

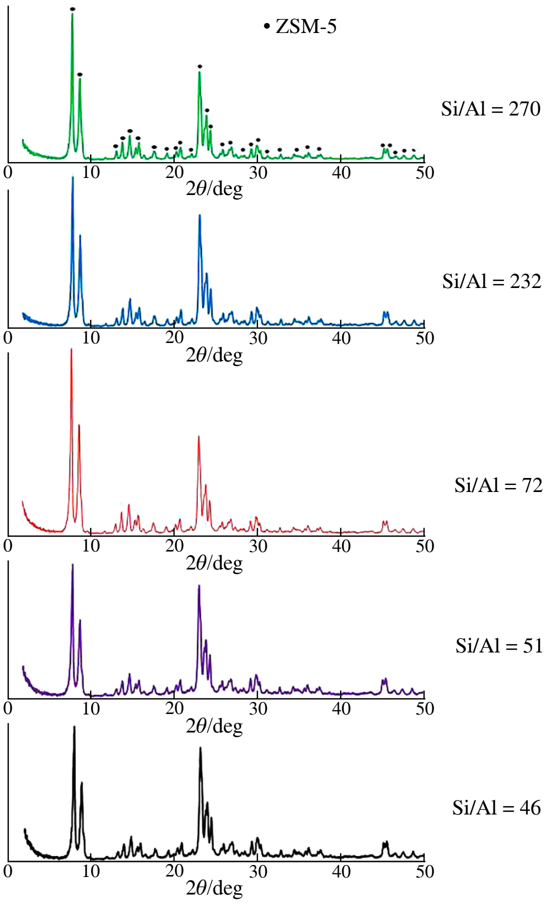

Figure 1 XRD patterns of synthesized nanosized ZSM-5 zeolites with different Si/Al ratios.

The particle sizes increase from 15–25 nm to 150 nm as the Si/Al ratio increases from 46 to 270 (Figure 2) in contrast to the data of earlier work,[28] where the authors recorded a decrease in the particle size with increasing Si/Al ratio. It was possible to establish the 'evolution' of the morphology of nanoscale zeolite HZSM-5 particles: aggregates in the form of 'tablets' with a diameter of 150 nm and a thickness of 80–100 nm consisting of small particles of 15–25 nm in size, their number increases with decreasing Si/Al ratio.

The characteristics of the specific surface area and porous structure of the synthesized samples are given in Table 2. All samples have a high specific surface area of 453–460 $m^2\,g^{-1}$. The external specific surface area increases with decreasing Si/Al ratio: 28 $m^2\,g^{-1}$ for a sample with the Si/Al ratios of 270 and 37 $m^2\,g^{-1}$ for samples with Si/Al ratios of 46 and 51, respectively. This is in good agreement with the SEM and TEM data, that reveal reducing the particle size with a decrease in the Si/Al ratio. It should be noted that the sample with the Si/A ratio of 51 possesses the best porous structure characteristics among all the samples (the largest pore volume, mesopore volume and external specific surface area).

Table 2 Textural properties of the synthesized nanosized HZSM-5 with different Si/Al ratios.

Sample	S_{BET}/ $m^2\,g^{-1}$	S_{ext}/ $m^2\,g^{-1}$	V_{total}/ $cm^3\,g^{-1}$	V_{micro}/ $cm^3\,g^{-1}$	V_{meso}/ $cm^3\,g^{-1}$
nanoHZSM-5_46	460	37	0.42	0.15	0.27
nanoHZSM-5_51	458	37	0.47	0.16	0.31
nanoHZSM-5_72	458	35	0.45	0.13	0.32
nanoHZSM-5_232	453	28	0.39	0.17	0.22
nanoHZSM-5_270	458	28	0.39	0.18	0.21

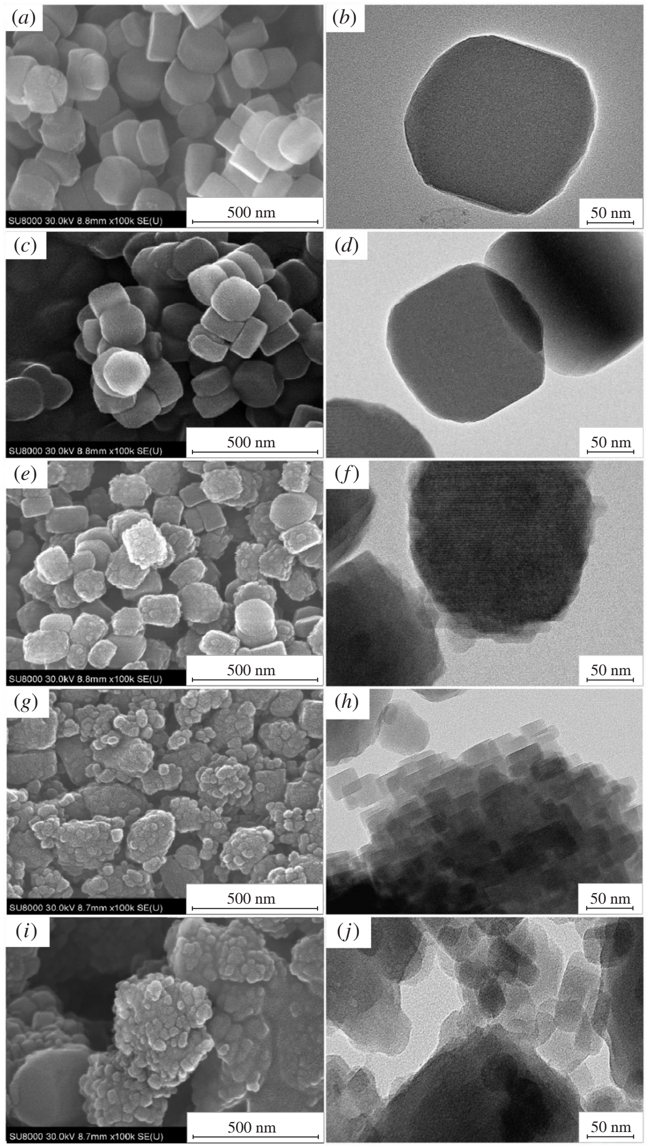

Figure 2 SEM and TEM images of the synthesized nanosized ZSM-5 zeolites with different Si/Al ratio: (*a*) and (*b*) Si/Al = 270; (*c*) and (*d*) Si/Al = 232; (*e*) and (*f*) Si/Al = 72; (*g*) and (*h*) Si/Al = 51; (*i*) and (*j*) Si/Al = 46.

The acidic properties of the synthesized samples were determined *via* the temperature-programmed desorption of ammonia (Table 3). All samples have a bimodal strength distribution of acid centers: weak and strong acid centers, respectively. Decrease in the Si/Al ratio results in the shift of the temperature peaks of desorption towards higher temperatures owing to an increase in the aluminum content in the zeolite framework. When the Si/Al ratio decreases

Table 3 Acidic properties of synthesized nanosized HZSM-5 zeolites with different Si/Al ratios.

Sample	T_{peak}/°C		Weak and medium strength[b]/ μmol g^{-1}	Strong acidity[c]/ μmol g^{-1}	Total acidity/ μmol g^{-1}
	LT peak[a]	HT peak[a]			
nanoHZSM-5_46	196	416	296	246	542
nanoHZSM-5_51	193	410	196	183	379
nanoHZSM-5_72	180	386	101	89	190
nanoHZSM-5_232	169	370	53	46	99
nanoHZSM-5_270	167	362	51	39	90

[a] The LT peak represents a low temperature desorption peak. The HT peak represents a high temperature desorption peak. [b] Calculated as the amount of NH_3 desorbed below 300 °C. [c] Calculated as the amount of NH_3 desorbed above 300 °C.

from 270 to 46, the total acidity increases by a factor of 6 – from 90 to 542 μmol g^{-1}. It should be noted that a slight predominance of weak acid centers is observed in all the samples.

In summary, the effect of the Si/Al ratio on the physicochemical properties (morphology, textural and acidic properties) of nanosized ZSM-5 zeolite synthesized by the one-stage microwave hydrothermal method directly in a proton form (HZSM-5) was studied for the first time. It has been found that the shape and particle sizes of synthesized nanosized HZSM-5 zeolites, as well as textural and acidic properties, have been largely depend on the Si/Al ratio. These data could allow one to obtain materials based on nanosized zeolites HZSM-5 possessing catalytic activity and stability.

This research was carried out with the financial support from the Russian Science Foundation grant no. 23-73-30007. Scanning electron microscopy characterization was performed in the Department of Structural Studies of Zelinsky Institute of Organic Chemistry, Moscow.

Online Supplementary Materials

Supplementary data associated with this article can be found in the online version at doi: 10.71267/mencom.7751.

References

1 S. Liu, S. Yang, J. He, D. Mao and C. Yin, *Inorg. Chem. Commun.*, 2021, **128**, 108564; https://doi.org/10.1016/j.inoche.2021.108564.

2 R. B. Lima, M. M. S. Neto, D. S. Oliveira, A. G. D. Santos, L. D. Souza and V. P. S. Caldeira, *Adv. Powder Technol.*, 2021, **32**, 515; https://doi.org/10.1016/j.apt.2020.12.030.

3 P. H. Hoang and N. T. T. Thao, *RSC Adv.*, 2022, **12**, 24511; https://doi.org/10.1039/D2RA04325D.

4 S. Wang, Z. Li, Z. Qin, M. Dong, J. Li, W. Fan and J. Wang, *Chin. J. Catal.*, 2021, **42**, 1126; https://doi.org/10.1016/S1872-2067(20)63732-9.

5 Z. Zhou, R. Jiang, X. Chen, X. Wang and H. Hou, *J. Solid State Chem.*, 2021, **298**, 122132; https://doi.org/10.1016/j.jssc.2021.122132.

6 A. Rashidvand, M. Kheirmand, B. Roozbehani and H. S. Hosseini, *Arabian J. Chem.*, 2023, **16**, 105330; https://doi.org/10.1016/j.arabjc.2023.105330.

7 Z. Jiang, D. Chen, W. Deng and L. Guo, *Chem. Phys. Impact*, 2022, **5**, 100134; https://doi.org/10.1016/j.chphi.2022.100134.

8 J.-H. Li, J.-Y. Xie, D. Zhang, L. Liu and J.-J. Xing, *J. Fuel Chem. Technol.*, 2021, **49**, 339; https://doi.org/10.1016/S1872-5813(21)60016-6.

9 A. Bayout, C. Cammarano, I. M. Costa, G. Veryasov, A. Sachse and V. Hulea, *J. Catal.*, 2024, **440**, 115828; https://doi.org/10.1016/j.jcat.2024.115828.

10 Y. Sun, T. Ma, L. Zhang, Y. Song, Y. Shang, Y. Zhai, Y. Gong and A. Duan, *Mol. Catal.*, 2020, **484**, 110770; https://doi.org/10.1016/j.mcat.2020.110770.

11 A. J. Mallette, S. Seo and J. D. Rimer, *Nat. Synth.*, 2022, **1**, 521; https://doi.org/10.1038/s44160-022-00091-8.

12 X. Mi, Z. Hou and X. Li, *Microporous Mesoporous Mater.*, 2021, **323**, 111224; https://doi.org/10.1016/j.micromeso.2021.111224.

13 Z. Xue, J. Ma, T. Zhang, H. Miao and R. Li, *Mater. Lett.*, 2012, **68**, 1; https://doi.org/10.1016/j.matlet.2011.10.019.

14 X. Chen, G. Yang and V. Valtchev, *Green Energy Environ.*, 2020, **5**, 394; https://doi.org/10.1016/j.gee.2020.10.014.

15 L. Chen, P. Lu, Y. Yuan, L. Xu, X. Zhang and L. Xu, *Chin. J. Catal.*, 2016, **37**, 1381; https://doi.org/10.1016/S1872-2067(15)61099-3.

16 B. Gehring, Y. Traa and M. Hunger, *Microporous Mesoporous Mater.*, 2021, **317**, 110978; https://doi.org/10.1016/j.micromeso.2021.110978.

17 J. Li, M. Liu, X. Guo, C. Dai and C. Song, *J. Energy Chem.*, 2017, **27**, 1225; https://doi.org/10.1016/j.jechem.2017.08.018.

18 S. Li, X. Ren, B. Mezari, Y. Liu, P. Pornsetmetakul, A. Liutkova, N. Kosinov and E. J. Hensen, *Microporous Mesoporous Mater.*, 2023, **351**, 112485; https://doi.org/10.1016/j.micromeso.2023.112485.

19 J. Li, M. Gao, W. Yan and J. Yu, *Chem. Sci.*, 2023, **14**, 1935; https://doi.org/10.1039/d2sc06010h.

20 L. Shirazi, E. Jamshidi and M. R. Ghasemi, *Cryst. Res. Technol.*, 2008, **43**, 1300; https://doi.org/10.1002/crat.200800149.

21 L. Yu, C. Xu, W. Zhang, Q. Zhou, X. Fu, Y. Liang, Z. Guo and W. Wang, *J. Solid State Chem.*, 2023, **327**, 124271; https://doi.org/10.1016/j.jssc.2023.124271.

22 J. Zhu, S. Yan, G. Xu, X. Zhu and F. Yang, *J. Solid State Chem.*, 2023, **318**, 123772; https://doi.org/10.1016/j.jssc.2022.123772.

23 M. A. Sanhoob, G. A. Nasser, A. I. Bakare, O. Muraza, T. K. Al-Shammari, H. V. Lee, T. Yokoi, S. Park and T. Nishitoba, *Arabian J. Sci. Eng.*, 2023, **48**, 16483; https://doi.org/10.1007/s13369-023-08417-0.

24 D. Si, M. Zhu, R. You, Y. Li, T. Wu, T. Gui, N. Hu, I. Kumakiri, X. Chen and H. Kita, *Microporous Mesoporous Mater.*, 2021, **324**, 111286; https://doi.org/10.1016/j.micromeso.2021.111286.

25 Y. Gao, B. Zheng, G. Wu, F. Ma and C. Liu, *RSC Adv.*, 2016, **6**, 83581; https://doi.org/10.1039/C6RA17084F.

26 H.-W. Huang, H. Zhu, S.-H. Zhang, Q. Zhang and C.-Y. Li, *J. Fuel Chem. Technol.*, 2019, **47**, 74; https://doi.org/10.1016/S1872-5813(19)30005-2.

27 X. Zeng, X. Hu, H. Song, G. Xia, Z.-Y. Shen, R. Yu and M. Moskovits, *Microporous Mesoporous Mater.*, 2021, **323**, 111262; https://doi.org/10.1016/j.micromeso.2021.111262.

28 Y. Hu, C. Liu, Y. Zhang, N. Ren and Y. Tang, *Microporous Mesoporous Mater.*, 2009, **119**, 306; https://doi.org/10.1016/j.micromeso.2008.11.005.

29 A. G. Dedov, A. A. Karavaev, A. S. Loktev, M. N. Vagapova, K. A. Cherednichenko, K. I. Maslakov, A. A. Sadovnikov and S. P. Molchanov, *Mendeleev Commun.*, 2024, **34**, 433; https://doi.org/10.1016/j.mencom.2024.04.039.

Received: 26th February 2025; Com. 25/7751